Ecological Modelling 495 (2024) 110802

Contents lists available at ScienceDirect

Ecological Modelling

journal homepage: www.elsevier.com/locate/ecolmodel

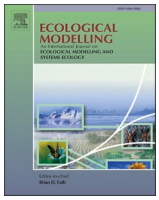

Site-level and spatially-explicit modelling provides some insights on key factors driving seasonal dynamics of an intertidal seagrass

Héloïse Muller [a,*], Etienne Auclair [a], Aubin Woehrel [a], Florian Ganthy [c], Pierre Tandeo [d], Paul Pao-Yen Wu [e], Carolyne Chercham [a], Martin Pierre Marzloff [b]

[a] IFREMER–DYNECO/DHYSED, Centre de Bretagne, CS1007 29280, Plouzané, France
[b] IFREMER–DYNECO/LEBCO, Centre de Bretagne, CS1007 29280, Plouzané, France
[c] IFREMER LER/AR, Quai du Commandant Silhouette, FR33120, Arcachon, France
[d] IMT Atlantique, Lab-STICC, UMR CNRS 6285 29238, France
[e] Queensland University of Technology, Mathematical Sciences School, 2 George Street, Brisbane, Australia

ARTICLE INFO

Keywords:
Seagrass meadows
Zostera noltii
Model coupling
Hydrodynamic model
Machine learning
Boosted regression trees
Arcachon bay

ABSTRACT

In a context of worldwide decline and given the critical ecological role of marine seagrasses to coastal ecosystem structure and functioning, regional conservation initiatives have emerged over the past thirty years to protect these important habitat-forming species. Yet, effective interventions need to account for site-specific processes and stressors. Thus, our ability to accurately predict seagrass dynamics is pivotal to support management interventions. To date, determinist process-based modelling has provided important insights on the drivers of seagrass dynamics. Here, we developed an original model framework that combines a coastal hydrodynamics ocean model with local data-driven models that rely on Boosted Regression Trees to predict seasonal dynamics of patch-level and plant-level seagrass features as a function of site-specific environmental conditions. Based only on a 12-month monitoring across nine sites, seagrass traits models successfully reproduce overall seasonal dynamics based mostly on inferred relationships with monthly light and temperature, and to a lesser extent, exposure to physical stressors (i.e., currents and waves). While models fail to finely capture spatial discrepancies across all sites (especially where seagrass demonstrates higher growth potential), spatially-explicit simulations highlight how seagrass-hydrodynamics feedback across the whole bay can dampen seagrass potential for growth due to exposure to shear stress. However, this original framework offers the potential to simulate long-term changes in the extent and status of seagrass meadows in Arcachon Bay, explicit resolving hydro-sediment dynamics effects on light appears as a priority to better capture the range of feedback processes between seagrass and coastal environmental conditions.

1. Introduction

Seagrasses, like other marine engineering species, have a key role in the structure and functioning of coastal ecosystems. They directly impact hydrodynamics and sediment dynamics by buffering waves (Gambi et al., 1990) and currents (Bos et al., 2007; Nordlund et al., 2017) and thus can effectively mitigate coastal erosion (Adriano et al., 2005; Falco et al., 2000; Ramage and Schiel, 1999). Seagrass meadows also offer important ecosystem services (Costanza et al., 1997) such as stabilizing local sediments (Waycott et al., 2009), acting as nursery and refuge habitats for species and promoting increases in biodiversity (Hughes et al., 2009), taking part in the carbon cycle by producing and storing carbon (Fourqurean et al., 2012) and being an edible resource for some species (Orth et al., 2006). Seagrass meadows strongly contribute to the structure of trophic networks and nutrient cycles (Hemminga and Duarte, 2000).

Similar to other intertidal habitat-forming species, seagrass meadows can vary in density and extent over multiple time scales in response to seasonal or interannual variability in environmental conditions or extreme events, and to anthropogenic stressors. They are under the influence of a broad range of environmental drivers including light availability, tidal and wind currents, waves, or temperature (Duarte, 1991; Fonseca and Bell, 1998; Auby et al., 1999; Massa et al., 2009; Balke et al., 2014). Seagrass decline has been globally documented

* Corresponding author.
E-mail address: heloise.muller@ifremer.fr (H. Muller).

https://doi.org/10.1016/j.ecolmodel.2024.110802
Received 14 November 2023; Received in revised form 9 July 2024; Accepted 10 July 2024
Available online 19 July 2024

across multiple regions and species (Waycott et al., 2009; Dunic et al., 2021; Turschwell et al., 2021) and can be attributed to several stressors (Orth et al., 2006) including: marine heatwaves, increased turbidity, poor water quality, sea level rise, diseases, coastal development or competition with other species. A meta-analysis of 215 published articles inferred a regression rate of 110 km^2 per year since the 1980s for all seagrass species and a 29 % loss of the known surface of seagrass meadows since the first measurements of seagrass distributions in 1980 (Waycott et al., 2009).

While several global studies have identified site-specific hazards (e.g. dredging or destruction by fisheries; Wu et al., 2017b; Krause-Jensen et al., 2021) that can explain contrasted trends in seagrass meadows across regions (e.g. Turschwell et al., 2021), a fine-scale understanding of the drivers of decline or recovery within individual sites often remain limited, albeit critical to support effective local management interventions. Amongst the numerous regional examples of global seagrass declines, on intertidal mudflats in Arcachon bay, southwestern France (Fig 1), the largest dwarf eelgrass (*Zostera noltii*) meadow in Europe (Auby et al., 2011) has dramatically declined over the past three decades (Fig 1) (Dalloyau et al., 2009; Plus et al., 2010; Lafon, 2013; Rigouin et al., 2022). Between 1989 and 2019, the total surface area of this meadow declined by 44 %, from 68,5 km^2 to 38,6 km^2. In the meantime, the eelgrass (*Zostera marina*), which also occurs in Arcachon Bay, along the subtidal edges of tidal channels, has decreased by 85 %, from 3,8 km^2 to 0,56 km^2 between 1989 and 2016. An initial decline in seagrass in the early 2000s, which is likely due to a heat wave episode as well as exposure to herbicides (Gamain et al., 2018), is assumed to have triggered a vicious cycle that involves complex feedback mechanisms between seagrass extent and density and hydro-sediment dynamics (Ganthy,2017; Cognat et al., 2018; Cognat, 2019; Fig 2). Specifically, *Z. marina* decline induced a subsequent increase in suspended sediment concentrations across the bay (Cognat et al., 2018) as well as muddy sediment accumulation in the upstream parts of Arcachon Bay. Seagrass regression induced a significant increase in both bottom currents, and waves in the whole Bay (Cognat, 2019), which could directly increase seabed erosion and the potential for shoot scouring or leaf tearing. Additional increase in turbidity directly reduced the amount of light available for photosynthesis, which reduced seagrass growth potential.

While feedback cycles between seagrass meadows and hydro-sedimentary conditions are well-identified as influencing long-term changes in Arcachon Bay, the relative contribution of individual processes (e.g., light, temperature, exposure to tidal-driven shear stress or to waves) to seagrass dynamics remains unknown. Such information is however critical to effectively guide conservation or restoration management interventions in the context of global changes. As a complementary approach to field observations and monitoring of seagrass meadows (Beca-Carretero et al., 2020) or to manipulative experiments (Burkholder et al., 1992; Short et al., 1995), modelling can offer unique insights on the processes that drive seagrass dynamics.

Both process-based and data-driven modelling approaches can help capture ecological dynamics and ecosystem-level responses to perturbations by accounting for complex interactions between biological and environmental processes that drive changes in coastal marine habitats. A broad range of modelling approaches types have been applied to assess and predict changes in *Zostera* spp. meadows including: statistical distribution models (Beca-Carretero et al., 2020), mechanistic distribution models (Greve and Krause-Jensen, 2005), seed dispersal models (Jahnke et al., 2016) or individual tracking of seeds (Kuusemäe et al., 2018), mechanistic growth model (Plus et al., 2003) and models for predicting the long term effects of environmental variables on spatial distribution of meadows (Ondiviela et al., 2014). Nevertheless, none of these models can fully capture the complex feedback cycles between seagrass dynamics, hydrodynamics and sediment processes across different temporal and spatial scales. While process-based approaches can account for these complex interactions between biological and physical components of coastal ecosystems (Ganthy et al., 2024), these data-hungry approaches are often limited by low data availability and high computational costs (Le Pevedic, 2024).

Here, so as to overcome technical constraints of existing modelling approaches, we developed a hybrid modelling framework, which combines (i) machine learning models and (ii) a spatially explicit coastal hydrodynamics model, to capture major interactions between seagrass and its hydro-sedimentary environment. (i) Boosted Regression Trees (BRT; Elith et al., 2008) were selected to predict monthly changes in six

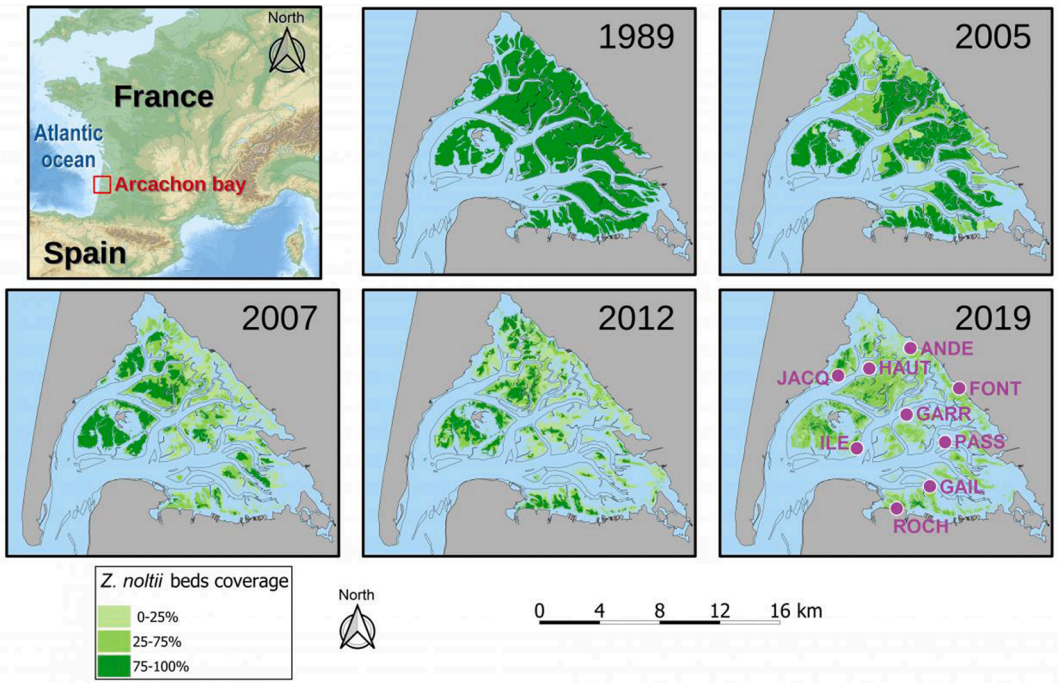

Fig. 1. Arcachon Bay's location and *Z. noltii* beds extents and coverage in 1989, 2005, 2007, 2012 and 2019. The nine sampling sites (ANDE, HAUT, FONT, JACQ, ILE, GARR, PASS, GAIL and ROCH) are plotted on the 2019 map.

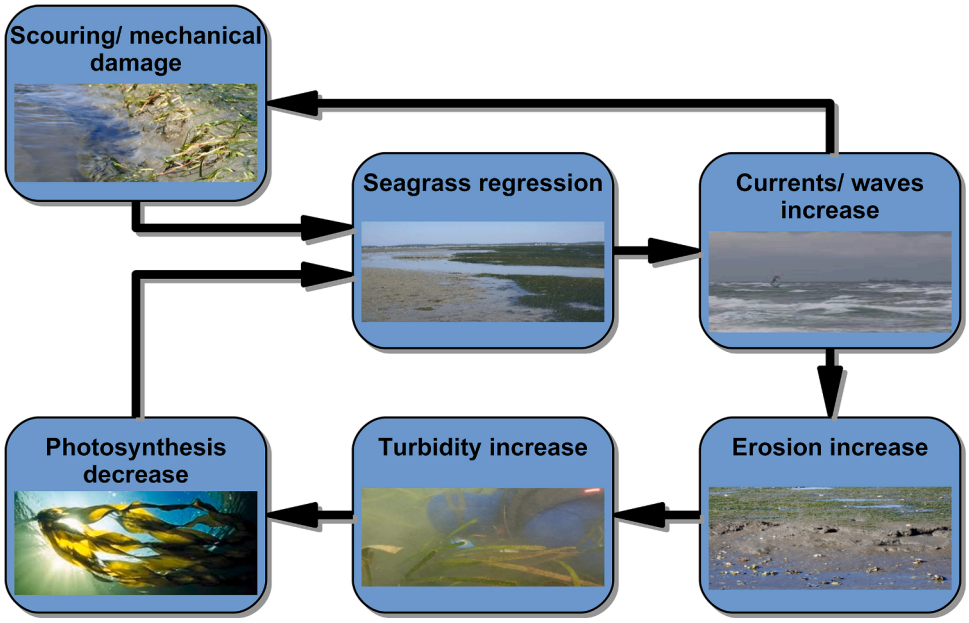

Fig. 2. Feedback processes between hydrodynamics, sediment dynamics and seagrass meadow development to illustrate the vicious cycle that can be triggered in response to seagrass regression (adapted from Cognat et al., 2019).

seagrass biological traits (e.g., leaf density, length or shoot height) with the associated uncertainties, as a function of local environmental conditions at several contrasted locations in the Bay (Cognat et al., 2018). BRT, which are particularly useful to model non-linear relationships, can perform on limited datasets (Elith et al., 2008). Using the permutation-importance heuristic (Linardatos et al., 2021), BRT can robustly estimate covariates importance to model predictions model, which facilitates model interpretation. (ii) The MARS3D coastal ocean model captures the plant-flow interactions (Kombiadou et al., 2014; Ganthy et al., 2024) to simulate the impacts of seagrass beds on hydrodynamics at the whole bay scale, which is relevant to study seagrass regional dynamics. Using this framework at both the level of individual seasonal monitoring sites and the scale of the whole Arcachon Bay, we explicitly modelled six patch-level (i.e. leaf biomass and density, root biomass) as well as plant-level (e.g. leaf length and width, shoot height) seagrass traits at two spatial scales in order to (i) assess the relative influence of local conditions (e.g. temperature, immersion time) versus hydrodynamics (e.g. exposure to shear stress, waves) to seagrass seasonal dynamics, and (ii) to better understand and predict seagrass spatial variability in Arcachon Bay.

2. Materials and methods

2.1. Context

2.1.1. Seagrass meadows in Arcachon bay

Arcachon Bay, located on the south French Atlantic coast (Fig 1), is a semi-enclosed mesotidal lagoon and 70 % of its surface is composed of mudflats. Due to its configuration, the Bay contains a network of tidal channels connecting the Bay to the Atlantic Ocean. Its hydro-sediment dynamics are driven by semidiurnal tide, freshwater inputs, swell and wind seas. Mean spring tidal range is 4,9 m and mean neap tidal range is 1,10 m (Cognat, 2019). Arcachon Bay contains two types of seagrass species both belonging to the *Zostera* genus: *Z. noltii* and *Z. marina*. *Z. noltii* is of small size (shoot height average: 9,5 cm, leaf width average: 1, 2 mm (Ribaudo et al., 2016)) and constitutes meadows on intertidal mudflats in Arcachon bay. In contrast, *Z. marina* (shoot height average: 76,25 cm, leaf width average: 6 mm (Cognat, 2019)) mostly colonizes shallow subtidal edges of tidal channels. The distribution of *Z. marina* meadows is not as widespread as that of *Z. noltii*. *Z. marina* and *Z. noltii* were mapped in Arcachon Bay in the summers of 1989, 2005, 2007, 2012, 2016 and 2019 (see Fig 1, Auby, 1991; Dalloyau et al., 2009; Plus et al., 2010; Lafon, 2013; Rigouin et al., 2022) using satellite and aerial data. However, seasonal field-based monitoring of meadows is only available for *Z. noltii* for the year 2016 (Cognat et al., 2018), which partially determined the focus on *Z. noltii* meadows for the seasonal growth data-driven model.

2.1.2. Data

2.1.2.1. Study site observations. Cognat et al. (2018) performed a monthly monitoring of biological and environmental parameters in *Z. noltii* meadows at nine intertidal sites (see Fig 1) of Arcachon Bay, between November 2015 and December 2016. This time period does not contain any particular events (extreme meteorological or pesticide release events) that could seriously impact the local seagrass dynamics. The nine sites were selected along different gradients across depth, environmental conditions and seagrass cover to represent overall variability in biological and environmental conditions in the Bay but they do not exhaustively capture seagrass meadows in the bay.

At each site, multiple environmental variables described in Cognat (2019), such as light received by plants (PAR for Photosynthetically Active Radiation), mean temperature (T_{mean}), average immersion time (Immersion) and wave exposure index (REIq75) were computed from high frequency measurements (every ten minutes) in order to obtain one value per month, i.e., per sampling of biological data. Regarding the biological data, the seagrass biological parameters (see Fig 3), leaf density which is the number of leaves per m^2 (Ldens, m^{-2}), leaf biomass (LBiom, $g.m^{-2}$), leaf length (Llength, m), leaf width (Lwidth, mm), shoot height (Sheight, m) and root biomass (RBiom, $g.m^{-2}$)) were indeed monthly monitored.

2.1.2.2. Coastal hydrodynamics model outputs. To complete the dataset, additional environmental parameters were computed thanks to the coastal hydrodynamic model MARS3D (Lazure and Dumas, 2008) which computes ocean physical variables (currents, free surface elevation, temperature and salinity) from the solutions of primitive equations under the hydrostatic approximation and the Boussinesq hypothesis. amongst the useful environmental parameters, a key parameter to

design the seagrass growth data-driven model is a theoretical metrics which is representative of potential leaf tearing or seagrass scouring F_{075}). F_{075} is built as the integral over time of the adimensional shear excess. The adimensional shear excess is expressed as f and stands for the excess of bottom current shear stress (τ_F) relative to the critical bed shear stress (τ_c) at which the leaves are torn off or scouring occurs.

$$F_{075} = \sum_{t=0}^{n} f(t)$$

With $f(t) = 0$ if $\tau_F(t) \leq \tau_c$

$f(t) = \frac{\tau_F(t)}{\tau_c} - 1$ if $\tau_F(t) > \tau_c$

And $\tau_F(t) = \frac{1}{2}\rho_{wat} C_D U_{bot}^2(t)$ where ρ_{wat} is the water density equal to 1023 $kg.m^3$, C_D is the drag coefficient equal to 1,5 and U_{bot} the bottom current.

τ_c is computed as τ_F by substituting U_{bot} by the critical bottom current fixed to 0,075 $m.s^{-1}$ (Cognat, 2019). MARS3D computes online the monthly value of F_{075} from the bottom current computed at a timestep of a few seconds on a 235-m grid. The MARS3D configuration is described in Cognat (2019) and Kombiadou et al. (2014). The 235-m 3D configuration is embedded in two successive 2D coarse resolution models which provide the sea surface height at its boundary condition. The initial 2D model is forced by the sea surface height from the FES 2012 global tidal model (Carrère et al., 2013). The whole modelling chain is forced with hourly meteorological parameters from the AROME weather model (Seity et al., 2011) and real river discharges. The seagrass effect on the waterflow is explicitly modelled in the hydrodynamics model configuration (Kombiadou et al. (2014) via the activation of a module called "obstruction" (Ganthy et al., 2024). Within this module, *Zostera* leaves are represented as rectangular parallelepipeds characterized by a length, a width, a thickness and a density per unit area, and can be curved according to their flexibility and the current intensity. During 3D computations, the drag effects and the modification of the turbulence around the leaves are taken into account through (1) momentum decrease because of the flow friction on the leaves and (2) the addition of sink and source terms in the turbulent closure scheme to take into account the turbulent kinetic energy modification and turbulence dissipation due to the seagrass presence.

The preliminary study of Cognat (2019) helped to choose respectively the environmental dataset composed of the data PAR, REIq75, *Tmean*, Immersion and *F*075 and the biological data composed of Ldens, LBiom, Llength, Lwidth, Sheight and RBiom as features and target data useful for the generic seagrass biological traits models (called the "local models" in the study) development with a machine learning approach.

2.2. Local model of monthly changes in six Z. noltii traits

2.2.1. Overall structure

In order to establish the local 1D seasonal growth model for *Z. noltii*, the knowledge of their past state is necessary to predict their new state. In practice, it means that the biological variables describing the seagrass (cf. Section 2.1.2) are used, at a previous time step, as features in a supervised machine learning algorithm in order to predict biological feature values for the next time step. It should be noted that some variables of the Cognat et al. (2018) dataset contain missing data due to field measurement issues on the first month of the survey in November 2015. Because duration between successive surveys varied from ~three to six weeks, the model is set to predict time-standardized (i.e. daily) rates of change for of the six biological features (see Fig 3a) of the seagrass meadows. These biological features monitored by Cognat et al. (2018) are useful for the parameterization of the obstruction in the coastal ocean model which will be used for the spatial model development. These predicted daily rates of change are then used to estimate the absolute values of the biological features at the next time step. Therefore, the original survey dataset was restructured into a usable dataset for the modelling, which contains for each of the nine sites, and each month of the year: daily rates of change for each of the six biological features, observed absolute values of each biological feature, and factors describing environmental conditions. The biological features and the environmental feature linked to hydrodynamics (F_{075}) were log-transformed to reduce skewness of data. As a result, the local growth model issued from the machine learning process and described on Fig. 3a, takes as inputs local environmental variables as well as the previous time-step biological feature (y_m) and predicts a daily variation of this biological feature (Δy_m) on a specific time range. The predicted variation (Δy_m) is then multiplied by the number of days (d) between two timesteps and is added to the previous biological value (y_m) in order to obtain an updated value (y_{m+1}).

$$\Delta y_m = f(y_m)$$

$$y_{m+1} = y_m + d \times \Delta y_m$$

f is the Boosted Regression Trees (BRT), m is month

A time-series of biological predictions is obtained by recurrently applying a local model using an initial biological value for the first-time step and then using the previous prediction as the new biological feature. The iteration process therefore simulates the local growth of *Z. noltii*, through all six biological traits (Ldens, Llength, LBiom, Lwidth, Sheight and RBiom), on a given period. The local models (one per biological traits) do not have explicit spatial and absolute time dimensions in themselves, since neither spatial coordinates nor time values are used as features. The spatial and time dimensions are inherent to the feature values given to the models as well as the choice of timesteps for the iterations.

2.2.2. Boosted regression trees

Within the context of Arcachon bay survey, the designed dataset composed of 108 observations corresponding to 12 months X 9 sites and 12 variables corresponding to all computed or measured environmental and biological parameters would not be enough to fit and test most of the existing learning methods that require large amounts of data. Therefore, BRTs were chosen based on their efficiency for the construction of the local model in terms of predictive performance, the interpretability of individual Regression Trees and appropriateness given the reduced amount of data available. Six independent local models were built, fitted and operated separately, to model each of the six biological variables of interest to predict seasonal changes in *Z. noltii* meadows properties. Each model is optimized by identifying the best set of three influential parameters, namely: the number of estimators (i.e. trees), the learning rate and the maximum depth. A grid search method is used to optimize each of the six BRTs. Grid searching consists in testing every possible combination of values of the three hyperparameters defined by an arbitrary grid of possible values to fit models and evaluate the performance of each model using cross-validation. We have chosen Root Mean Square Error (RMSE) as the metric to evaluate performance. It is used to select the best hyperparameters values. Since our dataset contains spatio-temporal data, it is important to take into account autocorrelation when choosing the folds of the cross-validation. Because of the absence of replicates at each sampling site and season, cross-validation folds can only take into account either the spatial or the temporal structure of our dataset. It was chosen to use group folds with each group corresponding to a sampling site in order to test the ability of the model to extrapolate through space. This choice of focusing on spatial group folds instead of time group folds makes the models better adapted to predict new seagrass meadow sites in 2016. This type of group fold consists in fitting a BRT on eight of the nine sampling sites and predicting the seasonal growth of the ninth site. The predicted and observed data are then used to compute the RMSE for this ninth site. The process is repeated for all other sites. Finally, the sets of optimal hyperparameters for the six BRT models are those minimizing the mean value of RMSE computed on test data of site-group-fold cross-validation.

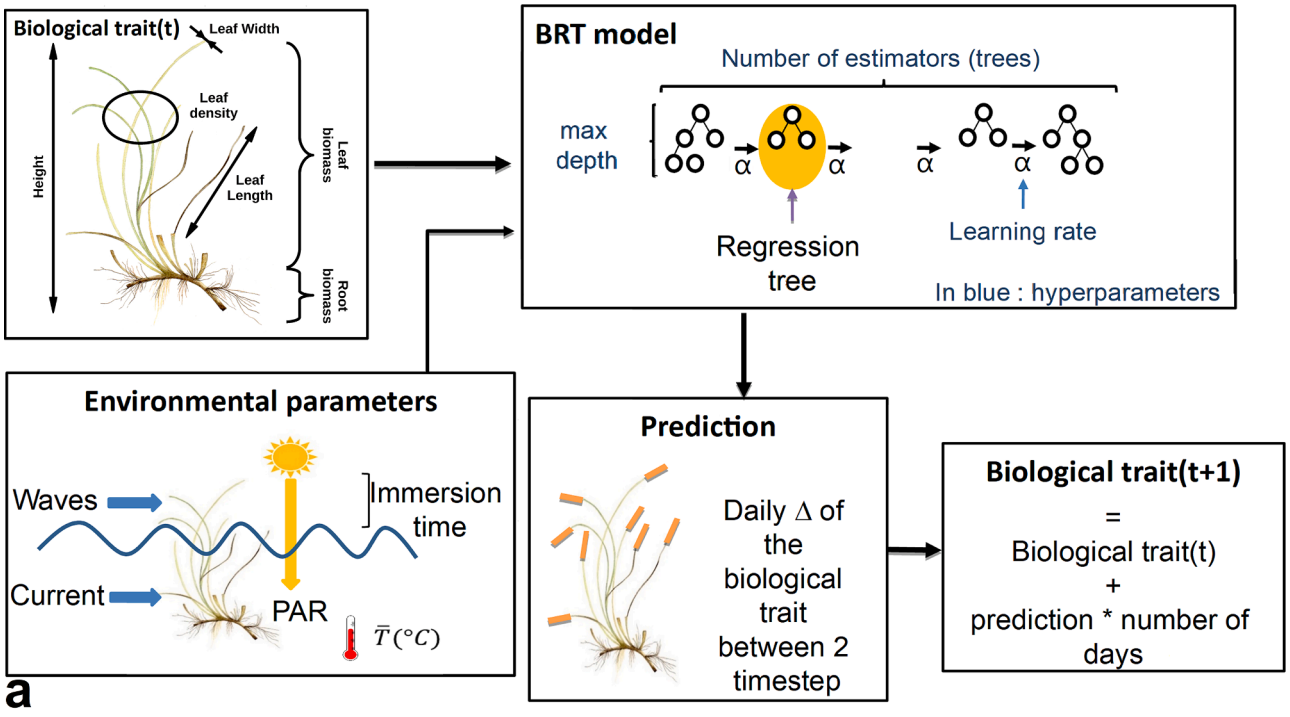

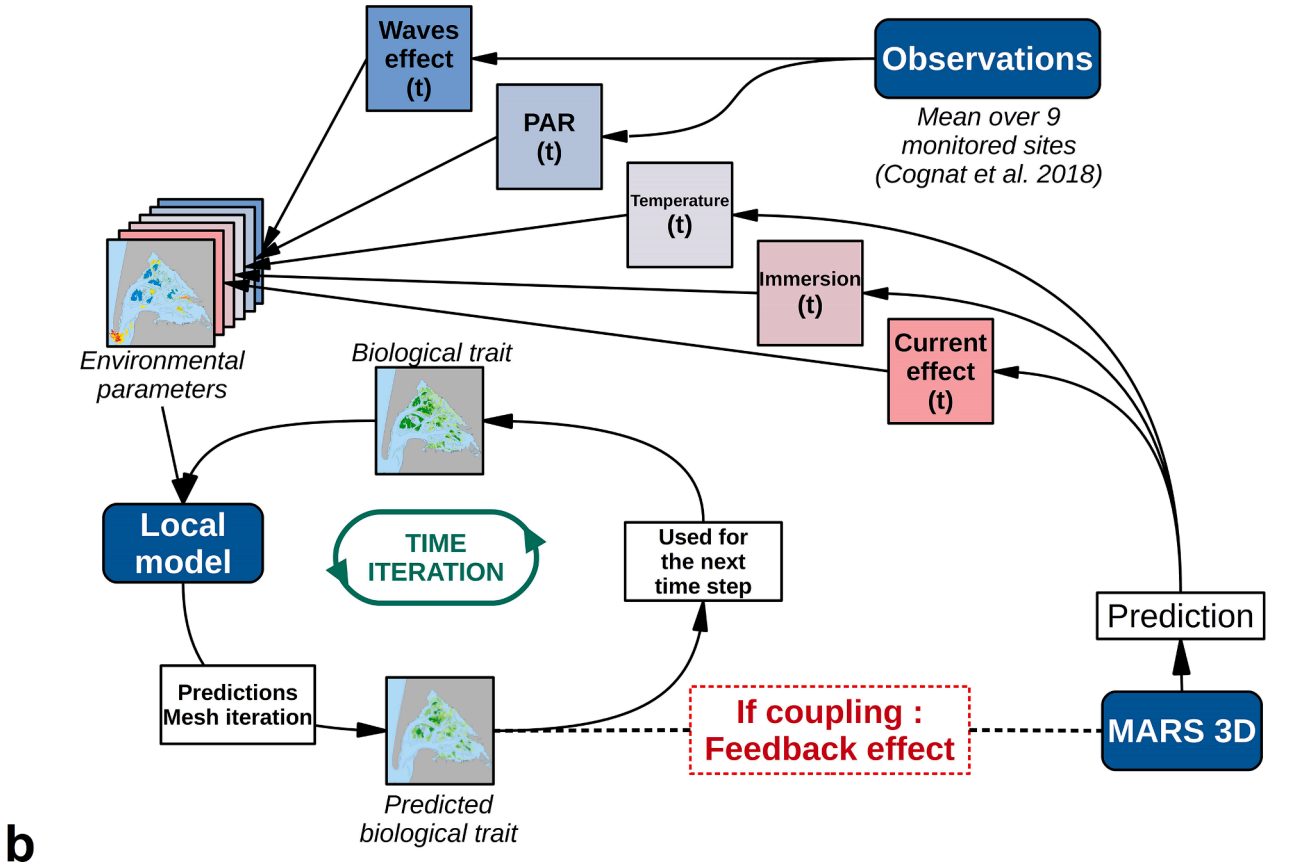

Fig. 3. Schematic representations of both (a) the local and (b) the spatially-explicit models structure. (a) The Boosted Regression Tree (BRT) models that predict local monthly changes in six seagrass traits, namely: leaf biomass, leaf density, leaf length, leaf width, root biomass and shoot height. Individual BRT models predict daily rates of changes in each of the seagrass traits as a function of the previous state of each trait as well as local environmental conditions (e.g. temperature, available light or Photosynthetic Available Radiation, Immersion time, exposure to waves and to tidal-driven shear stress). Estimated daily rates of change are then multiplied in the local model to predict changes over monthly time steps; (b) Spatialized model framework.

2.3. Spatial model

2.3.1. Hybrid model structure

The local models predict time series of the six biological variables that characterize *Z. noltii* meadows (Fig 3a). They are used to spatially predict changes in seagrass meadows using spatialized feature data. For this reason, in order to spatially predict the seasonal growth of *Z. noltii* meadows in the whole Arcachon Bay, a modelling framework combining the local BRT models with the MARS3D coastal ocean hydrodynamics model is developed. The spatially-explicit regional model framework for Arcachon Bay (Fig 3b) is structured according to a regular grid with a horizontal resolution of 235 m. Each cell of this grid is defined as a local spatial unit in which environmental and biological values are considered uniform. The MARS3D hydrodynamic numerical model predicts environmental feature values over this grid covering the whole Arcachon bay. A rasterized version of the 2016 distribution map of *Z. noltii* (Dalloyau et al., 2009) issued from the extrapolation of the available data (Fig 1), is used to obtain the presence/absence information of the species over the model computation grid. It enables to initialize grid cells for each biological feature of the meadows. For each of the biological features, the mean value of site-measured data of the first-time step from the 2016 survey (Cognat et al., 2018) is assigned, for the initial time, to each cell where the seagrass meadows were flagged as present in the presence/absence grid. The rest of the cells were assigned a value of 0. Then the local models fitted beforehand predict new biological values for each cell in the grid by iterating over the feature grids cell by cell. The results consist in spatialized predictions of the biological features at the next time step. Using the updated biological features grids and new environmental features grids predicted by MARS3D, this process is iterated at each time step to obtain a temporal succession of spatialized prediction grids of biological features. Therefore, the global model framework allows for obtaining spatio-temporal predictions of *Z. noltii* meadow's biological features.

2.3.2. Forcing vs. coupling mode

he MARS3D hydrodynamic numerical model has already been tested, validated and improved in Arcachon bay (Kombiadou et al., 2014; Ganthy et al., 2024) for environmental predictions. Therefore, in the architecture of the seagrass dynamics spatial model developed here, it is used to predict hydrodynamic environmental data, namely the Immersion time, F_{075} and temperature at a spatial resolution of 235 m. The model framework has two alternative pathways sharing common structure. The first pathway corresponds to a forcing model, where the computation of the environmental feature grids by MARS3D does not capture feedback between Zostera on its environment. This implies that the growth of the meadows depends on the previous biological and environmental values but the environmental features themselves do not depend on changes in *Z. noltii* meadows. The second pathway corresponds to a coupling model where the feedback effects of the meadows on their local environment are taken into consideration. In this case, the predicted biological features modify the environmental predictions made by MARS3D by modulating the amount of obstruction of bottom currents (described in part 2.1.2) and requires the features of *Z. noltii* to be contained in a grid usable by the model. The only environmental variable considered to account for the effects of hydrodynamics on seagrass development is the metrics F_{075} standing for the leaf tearing and seagrass scouring potentials (see part 2.1.2).

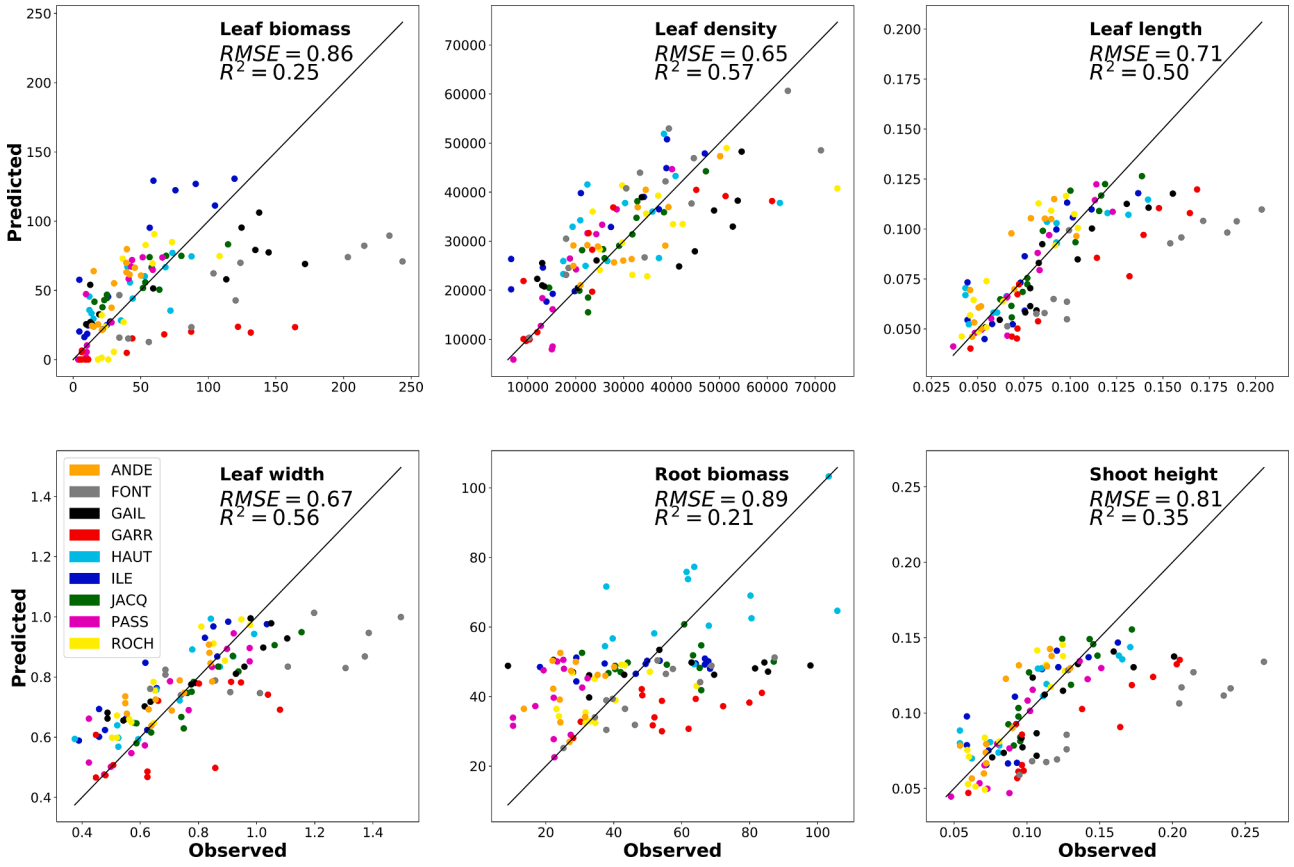

Fig. 4. Predicted vs observed monthly estimates for a full year, for each of the six individual BRT models (distinguished in the different panels as corresponding to the six seagrass features, namely Leaf biomass in g_{DW}/m^2, Leaf density in number of leaves/m^2, Leaf length in m, Leaf width in mm, Root biomass in g_{DW}/m^2, Shoot height in m). Each point corresponds to a given month for a given site (as colour-coded).

3. Results

3.1. Local model

Comparisons between monthly estimates of the six biological traits by the local models and site-specific observations (Fig 4) highlight the differences in model performance across the different seagrass traits and individual sites. Estimates by the leaf density model best match with observations (as indicated by the 0.57 correlation and the lowest Root Mean Square Error of 0.65; Fig 4), whereas variability in leaf biomass and root biomass are overall poorly estimated. While most models (e.g., leaf density; Fig 5) somehow capture the seasonal signal, monthly predictions for root biomass fail to track observed seasonal changes. This likely reflects that the environmental covariates fail to capture belowground drivers of seasonal changes. We do not further discuss root biomass predictions given low model performance and the fact that this trait is not required to parameterise obstruction in the hydrodynamics model.

In addition, whereas most models overall predict the seasonal range experience by seagrass traits across the different sites, high observed values at certain sites (e.g. GARR and FONT; Figs 4-5) are largely underestimated for most variables (leaf biomass, leaf density, leaf length, leaf width, shoot height). Fig. 5 illustrates these discrepancies in site-specific estimates for two patch-level seagrass traits (Leaf density, leaf biomass) across three contrasted locations (ROCH, FONT and GARR). For instance, ROCH, FONT and GARR are located, respectively, on the foreshore at the eastern end and at the southern end of the bay and on the edge of a channel in the middle of the bay (Fig 1).

Fig. 5 presents observed (dotted black line) and predicted (colour-coded solid lines) seasonal estimates for leaf density (top) and leaf biomass (bottom). A leave-one-out cross-validation was performed by fitting models on data collected at all sites but the one predicted. While Fig. 5 only displays one-year simulations, stability of model predictions was checked by running two-year simulations (under similar 2016 environmental conditions). For all sites, BRT model predictions for leaf density overall successfully reproduce the observed seasonal variability. Observed monthly leaf biomasses fall within the local model 95 % prediction interval at seven of the nine sites. For instance, at ROCH (bottom left panel in Fig 5), while predicted leaf biomass slightly underestimate winter observations, model predictions are in good agreement with spring-summer-autumn observations. Conversely, peak summer values observed at the GARR and FONT sites are largely underestimated. Similar results are obtained with the models for leaf density, shoot height, leaf length and leaf width (see Fig. 4).

Estimates of covariates importance to individual model predictions provide some insight on the key environmental factors driving seasonal changes in modelled seagrass traits (Fig 6). Specifically, variable importance estimates identify (i) standing values of modelled seagrass traits in the previous month, (ii) light availability (PAR) and mean site temperature as overall the most influential covariates contributing to the six independent BRT model predictions of daily rate of change in the considered features (Fig 6). The relative importance of temperature and light however varies across models: mean temperature largely contributes (>60 %) to model predictions for seagrass trait growth rates (i.e. leaf length and shoot height), while light availability is a relatively more influential covariate to predict seasonal changes in patch-level seagrass features (i.e. overall leaf biomass or leaf density) as well as leaf width. Note that model-derived covariates related to local hydrodynamics have a lesser influence to models predictions than light or temperature variables estimated from high frequency in situ monitoring, in particular: exposure to wave (REIq75) overall contributes by ~25 % to predictions of changes in leaf biomass (but only by ~6 % to other models). Potential for leaf tearing due to bottom shear stress (F_{075}) only influences predictions by ~6 % for both models associated with leaf density and leaf width (that both share similar modelled relationships with most covariates). Immersion time only contributes to predicted changes in leaf biomass (by ~6 %). Note that low influence of all covariates to predicted changes suggests that available covariates are irrelevant to capture variability in root biomass.

The Partial Dependence Plots (PDP; Fig 7) provide some further insights on modelled relationships between predicted changes in seagrass traits and monthly environmental conditions. For clarity, Fig. 7 exemplifies the nature of these relationships for only three models associated with changes in two patch-level (i.e. total leaf density on the top row and

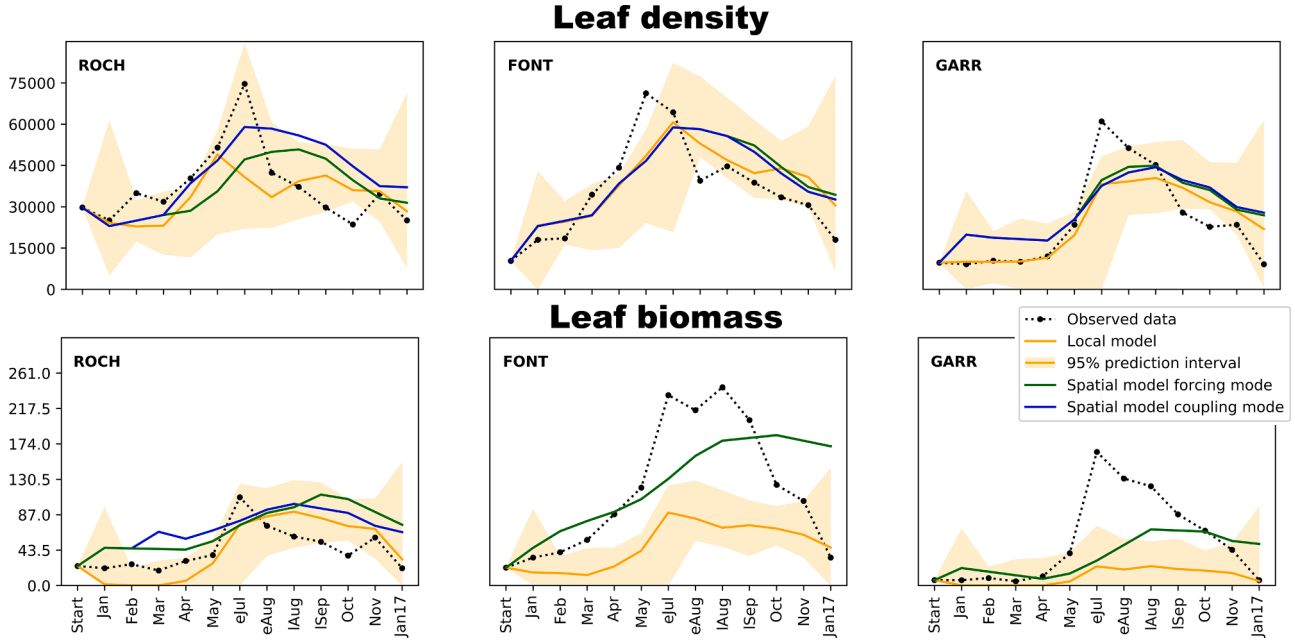

Fig. 5. Observed and predicted monthly estimates over 2016 for leaf density (top row, in number of leaves/m^2) and leaf biomass (bottom row, in g_{DW}/m^2) across three contrasted sites in Arcachon Bay. Sites code names are indicated in the top left of each subplot (see Fig. 1 for site locations). The labels in the X axis correspond to the date of the observed data (approximatively one observation per month at the middle of the month except for July, August and September where eJul stands for early July, eAug, for early August, lAug for late August and lSep for late September).

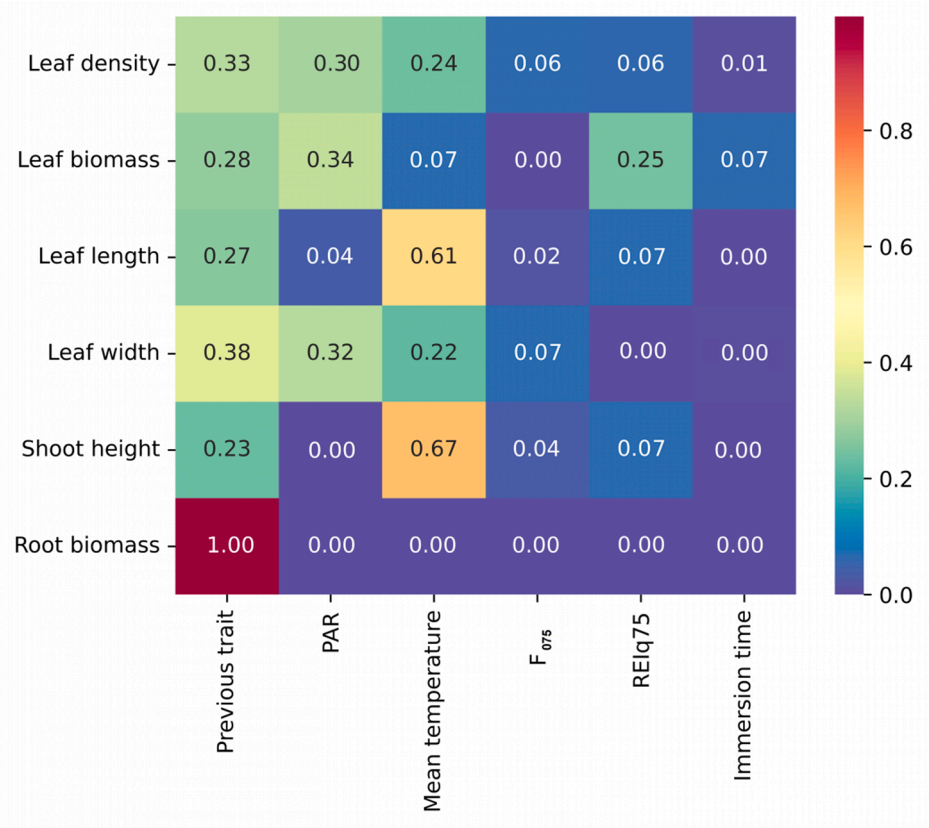

Fig. 6. Relative influence of the six covariates (as x-axis) to the six independent Boosted Regression Tree model predictions of daily rate of change in individual seagrass traits (as y-axis), i.e. Leaf density, Leaf biomass, Leaf length, Leaf width, Shoot height and Root biomass. Covariates include the modelled seagrass trait at the previous time step, light availability (i.e. PAR for Photosynthetically Active Radiation), mean temperature (that captures both air and sea conditions as recorded locally), potential for leaf tearing or seagrass scouring due to shear stress ($\boldsymbol{F}_{075}$), exposure to waves (REIq75), as well as mean immersion time.

total leaf biomass on the bottom row) and one plant-level (i.e. shoot height) seagrass traits. As observed across all six trait-specific models, rates of change are negatively related to the relevant traits (panels in the first column) in the previous month (here leaf density at the top, shoot height in the middle and leaf biomass at the bottom), which may capture mixed processes related to density-dependence and seasonal variability (i.e. maximum scope for growth at low density versus sharpest decline when seagrass reaches high leaf densities or individual sizes). Predicted increase in total leaf density (top row in Fig 7) mostly depends on availability of light, which partial effect becomes positive for PAR > 0.8 mol of photons/day/m^2 and optimal for PAR $>\sim 1.6$ mol of photons/day/m^2) and low to moderate temperatures (below 17 °C); high values of shear stress ($\log(F_{075}) > 1$) are detrimental to increase in leaf density. Conversely, mean temperature negatively influences change in mean shoot height below 12 °C, has a neutral influence on predictions at intermediate temperatures and becomes optimal when temperatures exceed 18 °C. Growth in shoot height is most facilitated by low shear stress conditions ($\log(F_{075}) < -5$). Predicted change in the other patch-level seagrass trait (i.e. total leaf biomass; bottom row) mostly depends on light availability, which positive effect follows similar thresholds as for leaf density; but the relative influence of other covariates on leaf biomass remains rather challenging to interpret.

3.2. Spatial model: forcing vs. coupling

The spatial model described in part 2.3, provides spatially-explicit monthly estimates for the six biological variables that characterize *Z. noltii* meadows, as illustrated in Fig 8. Both under forced or coupled simulations, estimates for all biological variables display similar spatial discrepancies that qualitatively match with known spatial dynamics in Arcachon Bay over a seasonal cycle. Seasonality is also well predicted by both frameworks as shown in Fig. 8, where leaf densities overall reach their peak values in August (2nd column). The greatest differences in spatial model predictions between coupled and forced model simulations (Fig 8, middle row) occur in the spring (1st column) and summer (2nd row) as the coupled simulation produces greater estimates of leaf densities (by ~5000 leaves per m^2) relative to the forced simulation on the inshore parts of the mudflats towards the upper end of the tidal channels. Besides, the coupling mode better captures autumn decline in seagrass leaf density in the back of the bay. Spatial differences in the computed potential for leaf tearing and seagrass scouring due to shear stress, are anticorrelated with differences in leaf density estimates between the coupling and forcing modes (Fig 8, bottom row), which overall reflects that lower leaf density estimates corresponds to higher current energy areas. Indeed, the coupled mode more finely estimates the local and bay-wide effects of seagrass distribution and status on hydrodynamics, which directly modulates seagrass growth in return. In mudflat areas neighbouring the major tidal channels, seagrass growth is lowered in the coupling mode relative to the forcing mode as exposed to higher potential for leaf tearing and seagrass scouring due to shear stress.

When extracting predicted leaf density and leaf biomass data at the nine sampling sites, coupled and forced simulations produce similar estimates of monthly changes in seagrass traits (close RMSE values, see table 1). However, as observed at the ROCH site (Fig. 5), occasional and marginal differences in monthly estimates suggest that coupled simulations may better capture local potential for growth (in the springtime) or decay (in the autumn). Predictions with both forced or coupled spatial models overall reproduce a smoother seasonal cycle than local model estimates at individual sites (Table 1) which overall results in larger

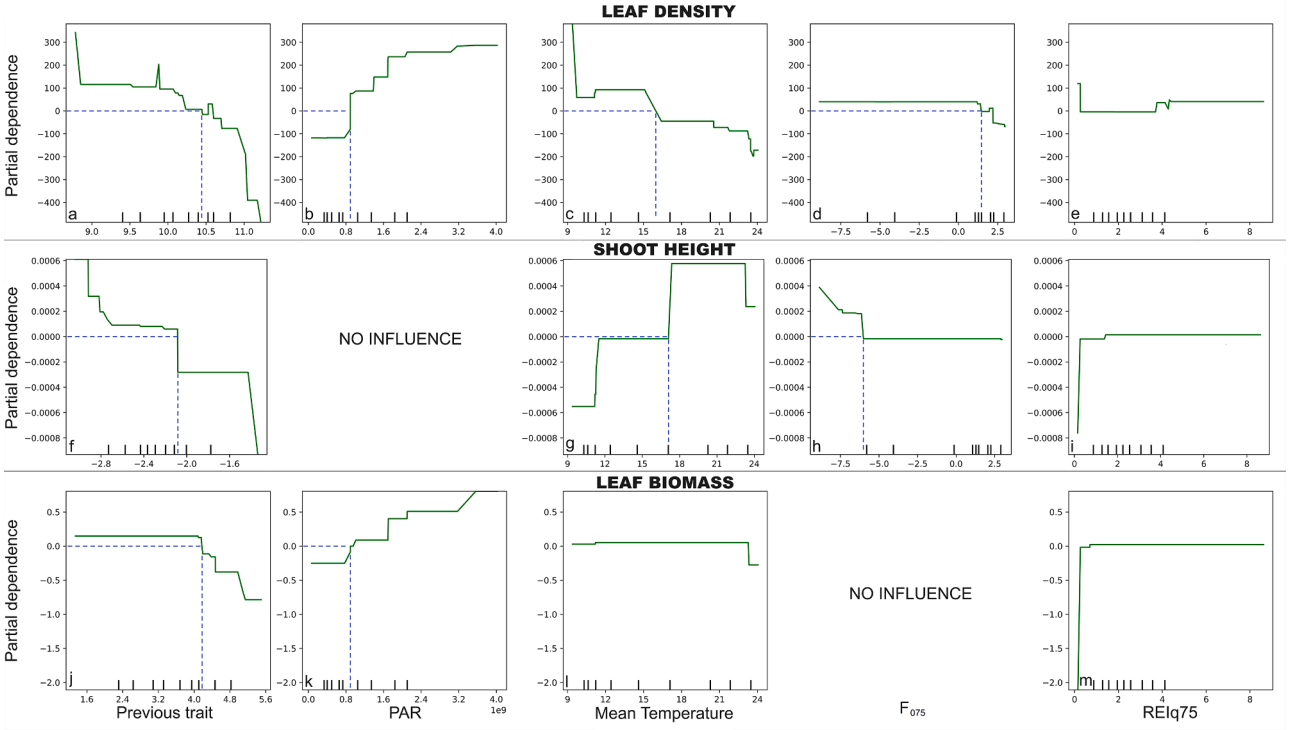

Fig. 7. Partial influence along the x-axes of (first column) modelled seagrass trait at previous time step (log-transformed), (2nd column) light availability (i.e. PAR in mol photons.$\boldsymbol{m}^{-2}$.$\boldsymbol{day}^{-1}$), (3rd column) mean monthly temperature (in °C), (4th column) potential for leaf tearing and seagrass scouring due to shear stress (expressed as log-transformed $\boldsymbol{F}_{075}$) or (5th column) due to waves (expressed as REIq75) on predicted daily changes in seagrass trait along the y-axis (i.e. leaf density on the top row; log-transformed shoot height on the middle row; and log-transformed leaf biomass on the bottom row).

RMSE (as highlighted in green in Table 1), except at the ILE or the GAIL sites where model predictions best match with observations using the coupled, or the forced spatial models, respectively. Note that light availability (i.e. PAR), which is the most influential environmental feature to predict leaf density (Fig 6), is assumed to be homogenous across the whole bay in the spatial model due to lack of spatially-explicit data, which may explain the relative homogeneity in leaf density monthly estimates across the nine monitoring sites.

Leaf biomass estimates are virtually identical in the forced and coupled simulations at the FONT and GARR sites. Note that, relative to the local model, both spatial models produce twice higher estimates for the high spring and summer biomass values, which somehow matches with observations. Such differences in leaf biomass estimates from spatial versus local models are likely mostly driven by discrepancies in mean temperature and immersion time covariates, which somehow influence leaf biomass prediction (see Fig. 7). Monthly values for these covariates are indeed estimated by the MARS3D coastal ocean model in the spatial-explicit simulations, as opposed to being sourced from in situ observations in non-spatial local model simulations.

4. Discussion

Several studies have documented and quantified the major drivers of seagrass decline at a global scale (Waycott et al., 2009; De Los Santos et al., 2019) as well as heterogenous trends in seagrass meadow status at a regional level (Turschwell et al., 2021; McMahon et al., 2022). However, site- and species-specific quantification of the local processes driving seagrass fine-scale dynamics are rather limited, except for correlative species distribution modelling studies (e.g. Adams et al. 2016a; Erftemeijer et al., 2023) that largely focus on projecting consequences of climate-driven or human-mediated changes. Understanding the role of fine-scale processes (acting at scales of 1–100 m) and predicting spatial and temporal changes in seagrass meadow at a local scale (from 10m-10 km) is however pivotal to inform effective spatial conservation or restoration management strategies in a context of global changes. In this paper, in order to better understand and predict the drivers of space-time variability in seagrass features across Arcachon Bay in southwestern France, we successfully developed a coupled seagrass-hydrodynamics model in a stepwise manner: first, local models of seasonal changes in six seagrass traits were fitted as a function of local environmental conditions across nine sites distributed over the whole of the bay; second, these local models coupled with a coastal ocean model allowed for the spatially-explicit modelling of seagrass-hydrodynamics feedback across the whole bay.

LOCAL MODELLING OF SIX SEAGRASS TRAITS SEASONAL DYNAMICS. Each of these modelling steps provides some complementary insights on drivers of seasonal and spatial variability in seagrass traits across Arcachon Bay. In the non-spatial site-specific models, temperature and light alongside with local site trajectories (i.e. the previous state of each trait) are the most influential covariates to Boosted Regression Tree (BRT) predictions of seasonal changes in seagrass traits, which is consistent with well-documented aspects of seagrass ecology. First, as a photosynthetic macrophyte, *Z. noltii* development largely depends on light availability (Cognat et al., 2018) and underwater light attenuation (Kombiadou et al., 2014; Plus et al., 2001, 2005). Moreover, temperature affects several physiological processes in seagrasses in general (Collier et al. 2017), and in *Z. noltii* in particular, including photosynthetic performance (Plus et al., 2005; Adams et al., 2016b) as well as respiration rates (Plus et al., 2001). While modelled trait-environment relationships can account for important non-linear effects, several of the inferred relationships appear rather as spurious correlation: the relationships between changes in leaf density (or biomass) and Photosynthetic Available Radiation (PAR; see Fig 8) capture meaningful ecological thresholds related to photosynthetic activity: from no development under low light conditions (PAR < 0.8 mol of photons/day/m^2), to a gradual increase in the potential for photosynthetic activity under

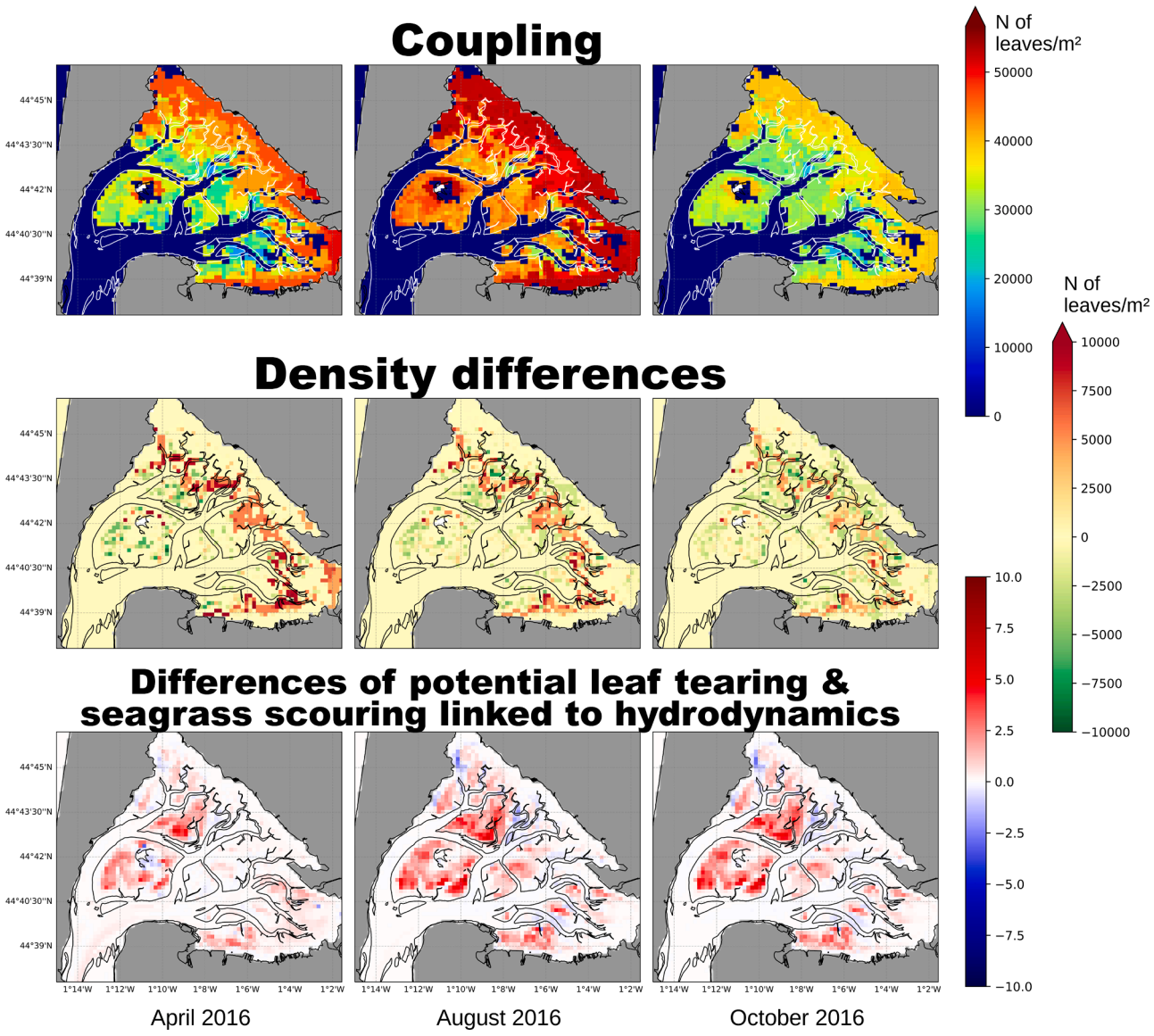

Fig. 8. Comparison between spatially-explicit model predictions of monthly leaf densities in April (1st column), August (2nd column) and October 2016 (3rd column) under a one-way forcing of seagrass dynamics versus a two-way coupling that captures seagrass-hydrodynamics feedback. The rows correspond respectively to monthly leaf density estimates from a two-way coupled seagrass-hydrodynamics simulation (top row), to differences in leaf densities between coupled versus forced simulations (middle row), and to differences in potential for leaf tearing and seagrass scouring due to shear stress (bottom row). Positive values correspond to greater values in the two-way coupling than in the one-way forcing.

intermediate light level; and up to an optimum under high light conditions. The relevance of these two light thresholds has been documented in experiments as well as based on expert elicitation (Hatum et al., 2022). However, inferred relationships related to exposure to waves, or to tidal-driven shear stress are rather weak and difficult to meaningfully interpret. Expectedly, monthly estimates of individual traits significantly contribute to predictions of seasonal changes, as these somehow capture the potential for increase in the winter months (when population or individual plant metrics are low), and conversely for decline in the late summer / autumn months (when traits reach their highest annual values).

Thus, unexpectedly and contrary to the initial assumptions that hydrodynamics constraints significantly dampen the potential for seagrass development in coastal ecosystems (Schanz and Asmus, 2003; Uhrin and Turner, 2018; Kalra et al., 2020; Risandi et al., 2023), and in Arcachon Bay in particular (Cognat 2019; Le Pevedic 2024), we only estimated a marginal influence of shear stress (i.e. F_{075} index) or exposure to waves (i.e. REIq75 index) on site-specific model predictions. Several reasons can explain this low contribution of hydrodynamics to predicted changes in seagrass traits. Scale mismatch between fine-scale changes in seagrass traits (observed within $0.5m^2$ quadrats), and coarse estimates of exposure to shear stress (at a 235 m horizontal model resolution), which biases estimated relationships with covariates (Mourguiart et al., 2024). Exposure to shear stress is also synthetised as a single expert-informed index (F_{075}), which simplifies time-integrated seagrass exposure to bottom shear stress over a month based on a set tolerance threshold (Cognat, 2019; Le Pelvedic, 2024). In this respect, further experimental work would be key to accurately assess seagrass tolerance thresholds to shear stress, or to wave exposure, and refine these thresholds. Importantly, model fitting was conducted on a single annual monitoring in 2016, which implies that, if local models overall reproduce mean 2016 seasonal changes in seagrass traits, they fail to capture interannual variability and larger changes in local hydrodynamics conditions (rather than within) in response to large bay-wide modification in seagrass distribution and status (for instance between 1990s and 2000s conditions, Fig. 1). Finally, rather than direct processes related to plant

Table 1
Normalized RMSE used to compare the predictions from the different models with the observations. Lowest RMSE scores for individual sites are highlighted in green to reflect which model configurations best matches with observations.

Model	SITES								
	ILE	HAUT	JACQ	GAIL	PASS	GARR	ROCH	FONT	ANDE
Local model	0,774	0,957	0,481	0,708	0,740	0,530	0,892	0,572	0,627
Spatial model forcing mode	0,697	1,117	1,129	0,688	0,807	0,618	0,968	0,697	1,741
Spatial model coupling mode	0,608	1,077	1,077	0,782	0,807	0,664	0,966	0,663	1,752

physical stress due to exposure to waves or tidal-driven shear stress, major effects of hydrodynamics on seagrass might mostly act indirectly via sediment resuspension (i.e. turbidity), which then induce some light-mediated effects on seagrass traits (as emphasised by Musavi et al. (2007)). Here, the model does not explicitly resolve spatial variability in light availability, which does appear as a priority for future model development given the high influence of light availability to model predictions for several seagrass traits.

PERFORMANCE OF THE MODELS. Patch-level metrics (i.e. total leaf biomass, leaf density and root biomass), which are most commonly reported and monitored, are not the most accurately predicted. For instance, root biomass is poorly predicted by the BRT. Conversely, plant-level traits (i.e. leaf length or width) which are necessary to parameterize the seagrass obstruction in the hydrodynamics model, are rather well-predicted with data-driven local models fed with light, temperature, waves, currents, immersion time and their past state in Arcachon bay. With regards to root biomass, which is poorly predicted but irrelevant to parameterise obstruction on the hydrodynamics, selecting a new set of predictors dedicated to below-ground processes (e.g. above-ground biomass, sediment types or deposition rates; Collier et al. (2021)) could improve model predictions.

While seasonal changes in most seagrass traits, in particular leaf density, leaf width, leaf length and shoot height, are well-captured by BRTs, spatial discrepancies across the bay, in particular at sites of higher potential for seagrass development, are underestimated. Thus, both collection of additional data across more sites as well as better characterising of local sites specificities will be key to consolidate models ability to mimic spatial variability in seagrass seasonal development. For instance, underestimating of maximum summer densities at certain sites could be due to not accounting for the presence of a thin water layer at that can help maintain high photosynthesis rates low tide (Cognat et al., 2018). More generally, downscaling model predictions to estimate changes in hydrodynamics conditions at a scale that better matches sampling resolution would also enhance models ability to capture ecologically meaningful relationships between seagrass traits and hydrodynamics conditions (Mourguiart et al.., 2024).

SPATIALLY-EXPLICIT MODELLING OF SEAGRASS-HYDRODYNAMICS FEEDBACK. While across the nine monitoring sites the relative influence of hydrodynamics is marginal, spatially-explicit modelling of seagrass-hydrodynamics feedback at the bay-wide scale produces meaningful spatial differences in seagrass seasonal dynamics. Modelling of biophysical interactions with submerged aquatic vegetation usually modifies seabed roughness and shear stress based only on plant biomass density estimates (Milbradt and Schonert, 2008; Kalra et al., 2020), whereas the proposed coupled framework finely captures the tridimensional obstruction and buffering of waves and currents by seagrass meadows (Ganthy et al. 2024; Le Pelvedic, 2024) based on multiple seagrass traits (i.e. leaf density, shoot height, leaf width and length). In the coupled relative to the forced simulations, higher shear stress on the mudflats most exposed to tidal-driven currents reduces the potential for seagrass density to build up. Conversely, when seagrass meadows are denser in the summertime, lower shear stress allows for the development of denser seagrass meadows in the upper parts of the mudflats near the upper ends of the tidal channels. However, the differences between coupling and forcing might be more contrasted with an interannual modelling which takes into account strong seagrass abundance changes induced by an extreme event.

While the coupled model finely captures some of the major processes involved in feedback loops between the coastal environment and seagrass meadows (in particular buffering of hydrodynamics by seagrass), the current framework, which can be updated as more data becomes available, offers several avenues for improvement. Indeed, with this modelling approach, we assumed plant physical stress due to exposure to waves or high tidal-driven bottom currents as a major effect of hydrodynamics on seagrass, whereas it is likely the indirect effect of hydrodynamics via sediment resuspension and light availability plays a greater role. Thus, given the relative importance of light (i.e. PAR) to predict changes in key seagrass traits, explicitly resolving spatial heterogeneity in light conditions across Arcachon bay appears as a definite priority. Indeed, a modification of the seagrass cover can impact light availability for seagrass which can impact the seagrass cover back. Developing a coupling between a hydro-sediment model that can explicitly simulate sediment dynamics, estimate turbidity and light received by seagrasses and the seagrass growth model would enable to model more properly the feedback processes and therefore help to provide long-term spatial predictions beyond the seasonal scale.

In this study, only local predictions were compared to observation but longer-term simulations issued from the spatial model could be assessed thanks to comparison with the seagrass percentage covers plotted on Fig. 1. The lateral growth also called the clonal growth could be included as an additional layer in the modelling framework: after the prediction of the seagrass growth in each cell, lateral growth rules could allow the colonization of neighbouring cells that do not contain seagrass meadows at the first timestep and also extinction of seagrass. The spatial rules could be based on thresholds of biological values at each cell to initiate colonization or extinction of a cell. Alternatively, to overcome data limitation, existing models using alternative framework that can rely on expert knowledge (e.g. Dynamic Bayesian Network; Wu et al.,

2017 a and b; Hatum et al., 2022) could be adapted to better capture hydrodynamics-related effects on seagrass. Such probabilistic modelling framework is also well-suited to capture ecological trajectories and associated uncertainties.

5. Conclusion

Thanks to Boosted Regression Trees, we successfully modelled the seasonal dynamics of multiple patch-level and plant-level seagrass traits, which allows for a detailed tridimensional representation of seagrass buffering effects on hydrodynamics (as opposed to most studies only considering shoot or leaf density/biomass). Nonetheless, even if hydrodynamics is known to directly determine seagrass dynamics via mechanical destruction, its influence is only secondary in local seagrass traits models. Thus, future work should consolidate the representation of the seagrass-hydrodynamics feedback by explicitly resolving sediment dynamics and flow-on effects on sediment stability, as well as turbidity and hence local light availability (one of the most important drivers identified in the local seagrass trait models) for seagrass photosynthesis. Capturing seagrass beds influence on sediment composition and its stabilization would also improve the description of the biophysical interactions in the model. Finally, the coupled model between a local model of a habitat-forming species and a coastal ocean model provides an original framework to understand and predict space-time variability, which could be transposed to other ecosystem or habitat-forming species (e.g. coral reefs, kelp beds).

CRediT authorship contribution statement

Héloïse Muller: Writing – review & editing, Writing – original draft, Supervision, Methodology, Investigation, Conceptualization. **Etienne Auclair:** Software, Investigation. **Aubin Woehrel:** Supervision, Investigation. **Florian Ganthy:** Methodology. **Pierre Tandeo:** Methodology, Conceptualization. **Paul Pao-Yen Wu:** Methodology, Investigation. **Carolyne Chercham:** Methodology. **Martin Pierre Marzloff:** Writing – review & editing, Methodology, Investigation, Conceptualization.

Declaration of competing interest

The authors declare the following financial interests/personal relationships which may be considered as potential competing interests: Muller Heloise reports was provided by IFREMER. If there are other authors, they declare that they have no known competing financial interests or personal relationships that could have appeared to influence the work reported in this paper.

Data availability

Data will be made available on request.

References

Adams, M.P., Saunders, M.I., Maxwell, P.S., Tuazon, D., Roelfsema, C.M., Callaghan, D. P., Leon, J., Grinham, A.R., O'Brien, K.R., 2016a. Prioritizing localized management actions for seagrass conservation and restoration using a species distribution model. Aquatic Conserv: Mar. Freshw. Ecosyst. 26, 639–659. https://doi.org/10.1002/aqc.2573.

Adams, M.P., Hovey, R.K., Hipsey, M.R., Bruce, L.C., Ghisalberti, M., Lowe, R.J., et al., 2016b. Feedback between sediment and light for seagrass: where is it important? Limnol. Oceanogr. 61, 1937–1955.

Adriano, S., Chiara, F., Antonio, M., 2005. Sedimentation rates and erosion processes in the lagoon of Venice. Environment International, Lagoon of Venice: loads, distribution, and effects of nutrients and pollutants 31, 983–992. https://doi.org/10.1016/j.envint.2005.05.008.

Auby, I., 1991. Contribution à L'étude Des Herbiers De *Zostera noltii* Du Bassin d'Arcachon: Dynamique, Production Et dégradation, Macrofaune Associée. Université Bordeaux 1.

Auby, I., Levavasseur, G., Plus, M., Deslous Paoli, J.M., Grillas, P., 1999. Comparaison Des Capacités Photosynthétiques Des Zostères Naines De Deux étangs méditerranéens: Lagune de Thau et étang du Vaccarès. Colloque "Le milieu aquatique: Interactions Des Facteurs Environnementaux Et Impacts Sur Les Organismes Vivants. Brest, 30 septembre –1 octobre 1999. http://archimer.ifremer.fr/doc/00152/26287/.

Auby I., Bost C.A., Budzinski H., Dalloyau S., Desternes A., Belles A., Trut G., Plus M., Pere C., Couzi L., Feigne C., Steinmetz J., 2011. Régression des herbiers de zostères dans le Bassin d'Arcachon: état des lieux et recherche des causes. RST/ODE/LER/AR/11.007. https://archimer.ifremer.fr/doc/00054/16507/.

Balke, T., Herman, P.M.J., Bouma, T.J., 2014. Critical transitions in disturbance-driven ecosystems: identifying windows of opportunity for recovery. J. Ecol. 102, 700–708.

Beca-Carretero, P., Varela, S., Stengel, D.B., 2020. A novel method combining species distribution models, remote sensing, and field surveys for detecting and mapping subtidal seagrass meadows. Aquatic Conservat. 30, 1098–1110. https://doi.org/10.1002/aqc.3312.

Bos, A.R., Bouma, T.J., de Kort, G.L.J., van Katwijk, M.M., 2007. Ecosystem engineering by annual intertidal seagrass beds: sediment accretion and modification. Estuar. Coast. Shelf. Sci. 74, 344–348. https://doi.org/10.1016/j.ecss.2007.04.006.

Burkholder, J., Mason, K., Glasgow Jr., H., 1992. Water-column nitrate enrichment promotes decline of eelgrass *Zostera manna*: evidence from seasonal mesocosm experiments. Mar. Ecol. Prog. Ser. 81, 163–178. https://doi.org/10.3354/meps081163.

Cognat, M., Ganthy, F., Auby, I., Barraquand, F., Rigouin, L., Sottolichio, A., 2018. Environmental factors controlling biomass development of seagrass meadows of *Zostera noltei* after a drastic decline (Arcachon Bay, France). J. Sea Res. 140, 87–104. https://doi.org/10.1016/j.seares.2018.07.005.

Carrère, L., Lyard, F., Cancet, M., Guillot, A., Roblou, L., 2013. FES 2012: a New Global Tidal Model Taking Advantage of nearly 20 Years of Altimetry. In: 20 years of progress in radar altimetry, symposium, 710. ESA (European Space Agency), Venice, Italy.

Cognat, M., 2019. Thèse de doctorat. Bordeaux.

Collier, C.J., Ow, Y.X., Langlois, L., Uthicke, S., Johansson, C., O'Brien, K., Hrebien, V., Adams, M.P., 2017. Primary productivity and thermal optima of three tropical seagrass species. Front. Plant Sci. 8, 1446.

Collier, C.J., Langlois, L.M., McMahon, K.M., Udy, J., Rasheed, M., Lawrence, E., Carter, A.B., Fraser, M.W., McKenzie, L.J., 2021. What lies beneath: predicting seagrass below-ground biomass from above-ground biomass, environmental conditions and seagrass community composition. Ecol. Indic. 121, 107156 https://doi.org/10.1016/j.ecolind.2020.107156. ISSN 1470-160X.

Costanza, R., d'Arge, R., de Groot, R., Farber, S., Grasso, M., Hannon, B., Limburg, K., Naeem, S., O'Neill, R.V., Paruelo, J., Raskin, R.G., Sutton, P., van den Belt, M., 1997. The value of the world's ecosystem services and natural capital. Nature 387, 253–260. https://doi.org/10.1038/387253a0.

Dalloyau S., Trut G., Plus M., Auby I., Emery E., 2009. Caractérisation de la qualité biologique des Masses d'Eau Côtières: cartographie des herbiers de *Zostera noltii* et *Zostera marina* du Bassin d'Arcachon. RST/LER/AR/09-003. https://archimer.ifremer.fr/doc/00167/27833/.

De los Santos, C.B., Krause-Jensen, D., Alcoverro, T., et al., 2019. Recent trend reversal for declining European seagrass meadows. Nat. Commun. 10, 3356. https://doi.org/10.1038/s41467-019-11340-4.

Duarte, C.M., 1991. Seagrass depth limits. Aquat. Bot. 40, 363–377. https://doi.org/10.1016/0304-3770(91)90081-F.

Dunic, J.C., Brown, C.J., Connolly, R.M., Turschwell, M.P., Côté, I.M., 2021. Long-term declines and recovery of meadow area across the world's seagrass bioregions. Glob. Change Biol. 27, 4096–4109. https://doi.org/10.1111/gcb.15684.

Elith, J., Leathwick, J.R., Hastie, T., 2008. A working guide to boosted regression trees. J. Animal Ecol. 77, 802–813. https://doi.org/10.1111/j.1365-2656.2008.01390.x.

Erftemeijer, P.L.A., van Gils, J., Fernandes, M.B., Daly, R., van der Heijden, L., Herman, P.M.J., 2023. Habitat suitability modelling to improve understanding of seagrass loss and recovery and to guide decisions in relation to coastal discharge. Mar. Pollut. Bull. 186, 114370 https://doi.org/10.1016/j.marpolbul.2022.114370. ISSN 0025-326X.

Falco, G.D., Ferrari, S., Cancemi, G., Baroli, M., 2000. Relationship between sediment distribution and *Posidonia oceanica* seagrass. Geo-Marine Lett. 1, 50–57.

Fonseca, M.S., Bell, S.S., 1998. Influence of physical setting on seagrass landscapes near Beaufort, North Carolina, USA. Mar. Ecol. Prog. Ser. 171, 109–121.

Fourqurean, J.W., Duarte, C.M., Kennedy, H., Marbà, N., Holmer, M., Mateo, M.A., Apostolaki, E.T., Kendrick, G.A., Krause-Jensen, D., McGlathery, K.J., Serrano, O., 2012. Seagrass ecosystems as a globally significant carbon stock. Nat. Geosci. 5, 505–509. https://doi.org/10.1038/ngeo1477.

Gambi, M.C., Nowell, A.R.M., Jumars, P.A., 1990. Flume observations on flow dynamics in *Zostera marina* (eelgrass) beds. Mar. Ecol. Prog. Ser. 61, 159–169.

Gamain, P., Feurtet-Mazel, A., Maury-Brachet, R., Auby, I., Pierron, F., Belles, A., Budzinski, H., Daffe, G., Gonzalez, P., 2018. Can pesticides, copper and seasonal water temperature explain the seagrass *Zostera noltei* decline in the Arcachon bay? Mar. Pollut. Bull. 134, 66–74.

Ganthy, F., 2017. Modification De L'asymétrie Tidale En Réponse à La Régression Des Herbiers De Zostères Dans Le Bassin d'Arcachon. EVOLECO - EVOlution à Long terme des Ecosystèmes COtiers: Vers une mise en évidence des forçages et des processus associés, Pessac, 5-7 décembre 2017.

Ganthy F., Verney R. and Dumas F., 2024. Improvements of a process-based model for 2- and 3-dimensional simulation of flow in presence of various obstructions. Available at SSRN: https://ssrn.com/abstract=4775274 or https://doi.org/10.2139/ssrn.4775274.

Greve, T.M., Krause-Jensen, D., 2005. Predictive modelling of eelgrass (*Zostera marina*) depth limits. Mar. Biol. 146, 849–858. https://doi.org/10.1007/s00227-004-1498-0.

Hatum, P.S., McMahon, K., Mengersen, K., Wu, P.-Y., 2022. Guidelines for model adaptation: a study of the transferability of a general seagrass ecosystem Dynamic bayesian networks model. Ecol. Evol. 12, e9172. https://doi.org/10.1002/ece3.9172.

Hemminga, M.A., Duarte, C.M., 2000. Seagrass Ecology. Cambridge University Press.

Hughes, A.R., Williams, S.L., Duarte, C.M., Heck, K.L., Waycott, M., 2009. Associations of concern: declining seagrasses and threatened dependent species. Front. Ecol. Environ. 7, 242–246. https://doi.org/10.1890/080041.

Jahnke, M., Christensen, A., Micu, D., Milchakova, N., Sezgin, M., Todorova, V., Strungaru, S., Procaccini, G., 2016. Patterns and mechanisms of dispersal in a keystone seagrass species. Mar. Environ. Res. 117, 54–62. https://doi.org/10.1016/j.marenvres.2016.04.004.

Kalra, T.S., Ganju, N.K., Testa, J.M., 2020. Development of a submerged aquatic vegetation growth model in the Coupled Ocean–Atmosphere–Wave–Sediment Transport (COAWST v3.4) model. Geosci. Model Dev. 13, 5211–5228. https://doi.org/10.5194/gmd-13-5211-2020.

Kombiadou, K., Ganthy, F., Verney, R., Plus, M., Sottolichio, A., 2014. Modelling the effects of *Zostera noltei* meadows on sediment dynamics: application to the Arcachon lagoon. Ocean. Dyn. 10, 1499–1516. https://doi.org/10.1007/s10236-014-0754-1.

Krause-Jensen, D., Duarte, C.M., Sand-Jensen, K., Carstensen, J., 2021. Century-long records reveal shifting challenges to seagrass recovery. Glob. Chang. Biol. 27, 563–575.

Kuusemäe, K., von Thenen, M., Lange, T., Rasmussen, E.K., Pothoff, M., Sousa, A.I., Flindt, M.R., 2018. Agent based modelling (ABM) of eelgrass (*Zostera marina*) seedbank dynamics in a shallow Danish estuary. Ecol. Modell. 371, 60–75. https://doi.org/10.1016/j.ecolmodel.2018.01.001.

Lafon, V., 2013. Cartographie de l'herbier à *Zostera noltii* du Bassin d'Arcachon par télédétection spatiale. Rapport final.

Lazure, P., Dumas, F., 2008. An external–internal mode coupling for a 3D hydrodynamical model for applications at regional scale (MARS). Adv. Water. Resour. 31, 233–250. https://doi.org/10.1016/j.advwatres.2007.06.010.

Le Pevedic, A., 2024. Thèse de doctorat. Bordeaux.

Linardatos, P., Papastefanopoulos, V., Kotsiantis, S., 2021. Explainable AI: a review of machine learning interpretability methods. Entropy 23 (1), 18. https://doi.org/10.3390/e23010018.

... & McMahon, K.M., Kilminster, K., Canto, R., Roelfsema, C.M., Lyons, M., Kendrick, G. A., Udy, J., 2022. The risk of multiple anthropogenic and climate change threats must be considered for continental scale conservation and management of seagrass habitat. Front. Mar. Sci. 9, 1–15. https://doi.org/10.3389/fmars.2022.837259.

Massa, S.I., Arnaud-Haond, S., Pearson, G.A., et al., 2009. Temperature tolerance and survival of intertidal populations of the seagrass *Zostera noltii* (Hornemann) in Southern Europe (Ria Formosa, Portugal). Hydrobiologia 619, 195–201. https://doi.org/10.1007/s10750-008-9609-4.

Milbradt, P., Schonert, T., 2008. A holistic approach and object-oriented framework for eco-hydraulic simulation in coastal engineering. Journal of Hydroinformatics 10 (3), 201–214. https://doi.org/10.2166/hydro.2008.029, 1 May 2008.

Mourguiart, B., Chevalier, M., Marzloff, M., Caill-milly, N., Mengersen, K., Liquet, B., 2024. Dealing with area-to-point spatial misalignment in species distribution models. Ecography IN PRESS. https://doi.org/10.1111/ecog.07104. Publisher's official version.

Musavi, M.T., Ressom, H., Srirangam, S., et al., 2007. Neural network-based light attenuation model for monitoring seagrass population in the Indian river lagoon. J. Intell. Inf. Syst. 29, 63–77. https://doi.org/10.1007/s10844-006-0031-y.

Nordlund, L.M., Koch, E.W., Barbier, E.B., Creed, J.C., 2017. Correction: seagrass ecosystem services and their variability across genera and geographical regions. PLoS. One 12. https://doi.org/10.1371/journal.pone.0169942.

Ondiviela, B., Losada, I.J., Lara, J.L., Maza, M., Galván, C., Bouma, T.J., van Belzen, J., 2014. The role of seagrasses in coastal protection in a changing climate. Coastal Eng., Coasts@Risks: THESEUS, A New Wave Coastal Protect. 87, 158–168. https://doi.org/10.1016/j.coastaleng.2013.11.005.

Orth, R.J., Carruthers, T.J.B., Dennison, W.C., Duarte, C.M., Fourqurean, J.W., Heck, K. L., Hughes, A.R., Kendrick, G.A., Kenworthy, W.J., Olyarnik, S., Short, F.T., Waycott, M., Williams, S.L., 2006. A global crisis for seagrass ecosystems. Bioscience 56, 987–996. https://doi.org/10.1641/0006-3568(2006)56[987:AGCFSE]2.0.CO;2.

Plus, M., Deslous-Paoli, J.M., Auby, I., Dagault, F., 2001. Factors influencing primary production of seagrass beds (*Zostera noltii Hornem.*) in the Thau lagoon (French Mediterranean coast). J. Exp. Mar. Biol. Ecol. 259 (1), 63–84. https://doi.org/10.1016/S0022-0981(01)00223-4. Publisher's official version.

Plus, M., Chapelle, A., Ménesguen, A., Deslous-Paoli, J.-M., Auby, I., 2003. Modelling seasonal dynamics of biomasses and nitrogen contents in a seagrass meadow (*Zostera noltii Hornem.):* application to the Thau lagoon (French Mediterranean coast). Ecol. Modell. 161, 213–238. https://doi.org/10.1016/S0304-3800(02)00350-2.

Plus, M., Auby, I., Verlaque, M., Levavasseur, G., 2005. Seasonal variations in photosynthetic irradiance response curves of macrophytes from a Mediterranean coastal lagoon. Aquat. Bot. 81 (2), 157–173. https://doi.org/10.1016/j.aquabot.2004.10.004.

Plus, M., Dalloyau, S., Trut, G., Auby, I., de Montaudouin, X., Emery, E., Noel, C., Viala, C., 2010. Long-term evolution (1988-2008) of *Zostera spp.* meadows in Arcachon Bay (Bay of Biscay). Estuarine Coastal Shelf Sci. 87 (2), 357–366. https://doi.org/10.1016/j.ecss.2010.01.016.

Ramage, D.L., Schiel, D.R., 1999. Patch dynamics and response to disturbance of the seagrass *Zostera novazelandica* on intertidal platforms in southern New Zealand. Mar. Ecol. Prog. Ser. 189, 275–288. https://doi.org/10.3354/meps189275.

Ribaudo, C., Plus, M., Ganthy, F., Auby, I., 2016. Carbon sequestration loss following Zostera noltei decline in the Arcachon Bay (France). Estuarine Coastal Shelf Sci. 179, 4–11. https://doi.org/10.1016/j.ecss.2016.01.024.

Rigouin L., Trut G., Bajjouk T., Rebeyrol S., Liabot P.O., Ganthy F., Auby I., 2022. Caractérisation de la qualité biologique des Masses d'Eau Côtières: cartographie des herbiers de *Zostera noltei* du Bassin d'Arcachon (MEC FRFC06 – Arcachon amont) par imagerie hyperspectrale. ODE/LITTORAL/LERAR/22.16. https://archimer.ifremer.fr/doc/00795/90675/.

Risandi, J., Rifai, H., Lukman, K.M., Sondak, C.F.A., Hernawan, U.E., Quevedo, J.M.D., Hidayat, R., Ambo-Rappe, R., Lanuru, M., McKenzie, L., Kohsaka, R., Nadaoka, K., 2023. Hydrodynamics across seagrass meadows and its impacts on Indonesian coastal ecosystems: a review. Front. Earth Sci. 11, 1034827 https://doi.org/10.3389/feart.2023.1034827.

Schanz, A., Asmus, H., 2003. Impact of hydrodynamics on development and morphology of intertidal seagrasses in the Wadden Sea. Mar. Ecol. Prog. Ser. 261, 123–134.

Seity, Y., Brousseau, P., Malardel, S., Hello, G., Bénard, P., Bouttier, F., Lac, C., Masson, V., 2011. The AROME-France convective-scale operational model. mon. Wea. Rev. 139, 976–991. https://doi.org/10.1175/2010MWR3425.1.

Short, F.T., Burdick, D.M., Kaldy, J.E., 1995. Mesocosm experiments quantify the effects of eutrophication on eelgrass, *Zostera marina*. Limnol. Oceanogr. 40, 740–749. https://doi.org/10.4319/lo.1995.40.4.0740.

Turschwell, M.P., Connolly, R.M., Dunic, J.C., Sievers, M., Buelow, C.A., Pearson, R.M., Tulloch, V.J.D., Cote, I.M., Unsworth, R.K.F., Collier, C.J., Brown, C.J., 2021. Anthropogenic pressures and life history predict trajectories of seagrass meadow extent at a global scale. In: Proceedings of the national academy of sciences of the United States of America, 118, pp. 1–11.

Uhrin, A.V., Turner, M.G., 2018. Physical drivers of seagrass spatial configuration: the role of thresholds. Landscape Ecol 33, 2253–2272. https://doi.org/10.1007/s10980-018-0739-4.

Waycott, M., Duarte, C.M., Carruthers, T.J.B., Orth, R.J., Dennison, W.C., Olyarnik, S., Calladine, A., Fourqurean, J.W., Heck, K.L., Hughes, A.R., Kendrick, G.A., Kenworthy, W.J., Short, F.T., Williams, S.L., 2009. Accelerating loss of seagrasses across the globe threatens coastal ecosystems. PNAS 106, 12377–12381. https://doi.org/10.1073/pnas.0905620106.

Wu, P.P.Y., McMahon, K., Rasheed, M.A., Kendrick, G.A., York, P.H., Chartrand, K., et al., 2017a. Managing seagrass resilience under cumulative dredging affecting light: predicting risk using dynamic Bayesian networks. J. Appl. Ecol. 55 (3), 1339–1350.

Wu, P.P.Y., Mengersen, K., McMahon, K., Kendrick, G.A., Chartrand, K., York, P.H., et al., 2017b. Timing anthropogenic stressors to mitigate their impact on marine ecosystem resilience. Nat. Commun. 8 (1), 1263.